PHYSICAL REVIEW B **77**, 220407(R) (2008)

Correlation between ferroelectric polarization and sense of helical spin order in multiferroic $MnWO_4$

Hajime Sagayama,[1] Kouji Taniguchi,[1] Nobuyuki Abe,[2] Taka-hisa Arima,[1] Minoru Soda,[3,*] Masato Matsuura,[3] and Kazuma Hirota[3,*]

[1]*Institute of Multidisciplinary Research for Advanced Materials, Tohoku University, Sendai 980-8577, Japan*

[2]*Department of Physics, Tohoku University, Sendai 980-8578, Japan*

[3]*The Institute for Solid State Physics, University of Tokyo, Kashiwa 277-8581, Japan*

(Received 22 April 2008; revised manuscript received 5 June 2008; published 30 June 2008)

We report a polarized-neutron-diffraction study on a single crystal sample of $MnWO_4$, wherein the ferroelectricity and spiral magnetic order coexist. The direction of electric polarization controls the sense of helix that can be detected from the difference in intensities of magnetic satellites for parallel and antiparallel spin directions of incident neutrons with respect to a scattering vector. The temperature dependence of the difference agrees well with that of the electric polarization. These results corroborate that an inverse effect of a Dzyaloshinskii-Moriya interaction is the origin of the spontaneous electric polarization in the spiral phase of $MnWO_4$.

DOI: 10.1103/PhysRevB.77.220407 PACS number(s): 75.80.+q, 61.05.F−, 77.80.Fm

Recently, a strong interplay between ferroelectric polarization (P) and magnetic order has been found in multiferroic materials.[1] Especially, the electric control of spin helicity[2] and the magnetic control of electric polarization[3–6] in perovskite $RMnO_3$ (R=Tb or Dy) are worthy of special attention. In these compounds, magnetic frustration results in a nontrivial long-wavelength magnetic order. Spontaneous electric polarization occurs as the magnetic structure changes from a collinear sinusoidal one to a transverse cycloidal spiral one.[7,8] Polarization has been found to be largely affected by the application of a magnetic field, possibly due to the fragile long-wavelength magnetic structure of the frustrated magnetic systems. Some models representing the coupling between a spin system and electric polarization have been proposed.[9–13] According to Katsura *et al.*,[9] a noncollinear arrangement of two adjacent spins $\boldsymbol{S}_i$ and $\boldsymbol{S}_j$ can produce a local electric polarization $\boldsymbol{p}_{ij}$, which can be expressed as

$$\boldsymbol{p}_{ij} = A\boldsymbol{e}_{ij} \times (\boldsymbol{S}_i \times \boldsymbol{S}_j), \tag{1}$$

with $\boldsymbol{e}_{ij}$ being the unit vector connecting the sites i and j. A is a coupling constant related to spin-orbit coupling and spin-exchange interaction. $\boldsymbol{S}_i \times \boldsymbol{S}_j$ is usually referred to as spin-vector chirality. Polarization with the same expression is also expected from the inverse Dzyaloshinskii-Moriya (IDM) interaction.[10] Yamasaki *et al.*[2] have confirmed the correlation between the spin chirality and the spontaneous electric polarization in $TbMnO_3$ by using a polarized-neutron-diffraction technique. The helicity of a cycloidal spin structure is found to be switched by the reversal of the electric polarization. The IDM mechanism is considered to be applicable to several other spiral multiferroics.[14–20]

In this Rapid Communication, we report the spin-polarized-neutron-diffraction study of a prototypical magnetoelectric multiferroic material $MnWO_4$. It crystallizes in a monoclinic wolframite structure with a space group $P2/c$, as shown in Fig. 1(a) (Ref. 21). The values of lattice constants a, b, c, and β are 4.82 Å, 5.75 Å, 4.99 Å, and 91.075°, respectively. Each unit cell includes two Mn^{2+} ions at $\boldsymbol{r}_1 = (0.5, y, 0.25)$ and $\boldsymbol{r}_2 = (0.5, 1-y, 0.75)$ with y=0.685; the ions are interconnected via the common edges of distorted MnO_6 octahedra and form zigzag chains along the c axis. A relatively weak nearest-neighbor superexchange via the bending of Mn-O-Mn bonds competes with other Mn-O-O-Mn superexchange interactions, inducing successive magnetic phase transitions at 13.5 K (T_N), 12.7 K (T_2), and 7.6 K (T_2) (Refs. 21 and 22). Sinusoidally modulated collinear antiferromagnetism is stable in the antiferromagnetic AF3 phase ($T_2 < T < T_N$) with wave vector $\boldsymbol{k}$=(−0.214, 1/2, 0.457). The magnetic moments of Mn^{2+} align along the easy axis that lay in the ac plane forming an angle of α=34° with the a axis, as shown in Fig. 1(b). Accompanied by a second-order-like phase transition at T_2, an additional component of the ordered magnetic moment along the b axis appears in the AF2 phase ($T_1 < T < T_2$), resulting in a helical spin structure with $\boldsymbol{k}$ almost identical to that in AF3. The magnetic structure in the AF1 phase below T_1 again becomes collinear but with a commensurate wave vector $\boldsymbol{k}$=(−1/4, 1/2, 1/2). Spontaneous electric polarization along the b axis occurs only in the spiral AF2 phase,[23,24] suggesting that a noncollinear spin configuration plays a key role in the occurrence of

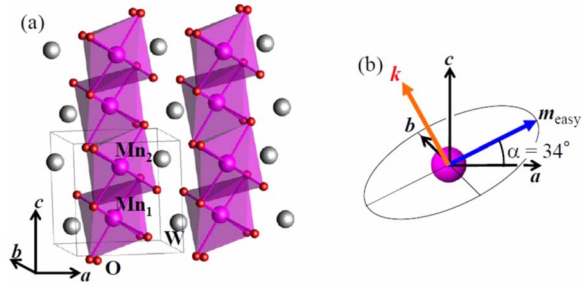

FIG. 1. (Color online) (a) The crystal structure of $MnWO_4$. The unit cell is indicated by the thin solid lines. The edge-sharing MnO_6 octahedra form zigzag chains along the c axis. (b) The basal plane of the spiral spin structure in the ferroelectric phase of $MnWO_4$. The easy spin direction forms angle α=34° with the a axis. The direction of the magnetic wave vector $\boldsymbol{k}$ is also indicated.

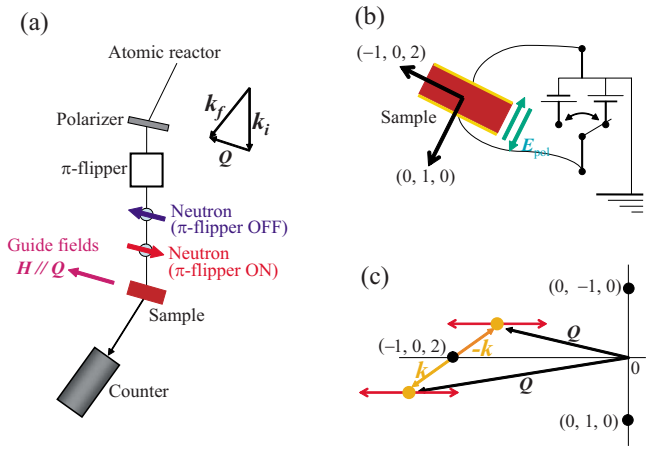

FIG. 2. (Color online) (a) A schematic top view of the PONTA spectrometer for conducting the neutron scattering experiment in the two-axis mode. Up-spin neutrons diffracted by the Heusler alloy pass through a π flipper. The neutron spin is gradually rotated to parallel or antiparallel with respect to Q. (b) The scattering plane is normal to the [2 0 1] axis. A poling electric field is applied parallel ($E_{\mathrm{pol}}>0$) or antiparallel ($E_{\mathrm{pol}}<0$) to the b axis. (c) The projected traces of Q scans of the two magnetic satellites $(-1,0,2)\pm k$ are denoted by arrows in the scattering plane.

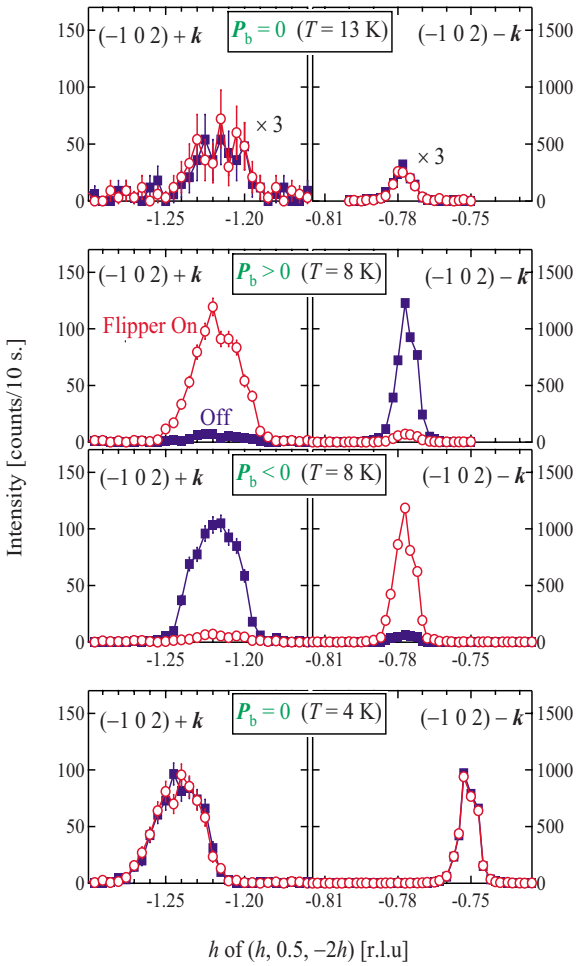

FIG. 3. (Color online) The Q-scan profiles of the magnetic satellites $(-1,0,2)\pm k$ in the spiral phase (AF2) and the collinear antiferromagnetic phases (AF1 and AF3).

electric polarization. The IDM effect is the prime candidate for the origin of ferroelectricity. In order to quantitatively compare the ferroelectric polarization and the spin-vector chirality in $MnWO_4$, we have performed spin-polarized-neutron-diffraction measurements. The analysis of the ellipticity of the helix has revealed a contrasting behavior that of $TbMnO_3$.

The spin-polarized-neutron-diffraction measurements were performed with a polarized neutron triple-axis spectrometer (PONTA) at Japan research reactor 3 (JRR-3) in Japan. Figure 2(a) illustrates a schematic top view of the spectrometer in the two-axis mode of operation for the measurements. Details regarding the spin-polarized-neutron-diffraction measurements have been described elsewhere.[2] The spin polarization of the incident neutrons defined as the difference between the probabilities of up- and down-spin neutrons was 0.9. A single crystal of $MnWO_4$ was grown by using a floating-zone method. The crystal was shaped into a short cylinder with a diameter of 3 mm and height of 2.5 mm. Gold electrodes were deposited onto the wide faces of (0,1,0) shown in Fig. 2(b). The sample was mounted on a sapphire plate in a closed-cycle ^{4}He refrigerator and irradiated with a spin-polarized neutron beam. All the neutron diffraction measurements were performed without the application of an electric field after cooling the sample from 20 K in a poling field (± 80 kV/m) strong enough to saturate the electric polarization. The peak profiles of a pair of magnetic satellites at $(-1,0,2)\pm\boldsymbol{k}$ were measured along the $(-1,0,2)$ direction in the reciprocal space shown in Fig. 2(c). Integrated intensities were corrected by taking into account the incomplete polarization of the incident neutron beam. The temperature dependence of electric polarization P_b was calculated from a pyroelectric current measured in a warming run without the application of an electric field by using an electrometer after cooling in the same poling field as that used in the neutron diffraction measurements.

Figure 3 presents the profiles of the magnetic satellites at different temperatures. The intensity (I_{ap}) of satellite $(-1,0,2)+\boldsymbol{k}$ for a positively poled ferroelectric state ($P_b>0$) with the neutron spin ($\boldsymbol{S}_n$) antiparallel to a scattering vector $\boldsymbol{Q}$ (I_{ap}) became 25 times as large as that (I_p) with $\boldsymbol{S}_n$ parallel to $\boldsymbol{Q}$ (I_p). As for the other satellite, $(-1,0,2)-\boldsymbol{k}$, conversely I_p was considerably higher than I_{ap}. These behaviors are expected in the case of a helical magnet.[25] In the case of $P_b<0$, these relations between the intensities were reversed. This indicated that the sense of helix, referred to as the spin chirality could be controlled by poling the electric fields, as in the case of $TbMnO_3$ (Ref. 2). The difference in the intensities disappeared in the paraelectric phases, AF1 and AF3, resulting to one of the collinear spin alignment.

The chirality of the helix was determined as follows. In $MnWO_4$ the magnetic moment $\boldsymbol{M}_{\alpha l}$ on site $\boldsymbol{r}_\alpha$ ($\alpha=1$ or 2) in cell l at $\boldsymbol{R}_l$ can be described as

$$\mathbf{M}_{\alpha l}=\mathbf{m}_{\mathrm{easy}}\cos(2\pi\mathbf{q}\cdot\mathbf{R}_l+\phi_\alpha)+\mathbf{m}_b\sin(2\pi\mathbf{q}\cdot\mathbf{R}_l+\phi_\alpha), \tag{2}$$

where $\phi_2=\phi_1+\pi(q_z+1)$ (Ref. 21). The amplitudes of the easy axis ($\boldsymbol{m}_{\mathrm{easy}}$) and b-axis ($\boldsymbol{m}_b$) components of the helix

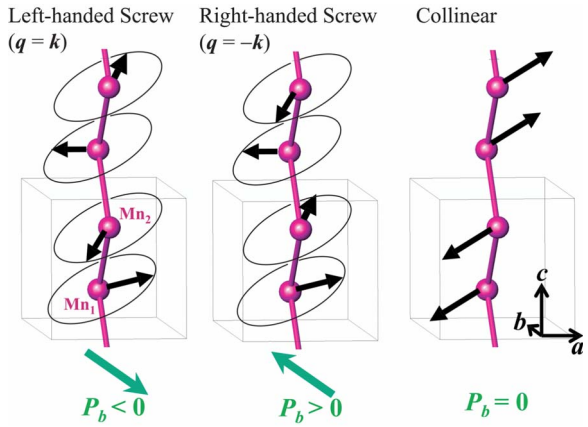

FIG. 4. (Color online) The relation between electric polarization and spin structure. The left- and right-handed screw configurations on a zigzag chain correspond to the $P_b>0$ and $P_b<0$ states, respectively.

have been reported to be ~4.5 μ_B at 9 K through a magnetic structure analysis. The propagation vector $\boldsymbol{q}$ was defined as $\boldsymbol{q}=\boldsymbol{k}$ and $\boldsymbol{q}=-\boldsymbol{k}$ when the sense of the helix was parallel and antiparallel to $\boldsymbol{k}$, respectively. Note that the sense of helix corresponded to the spin chirality. This magnetic modulation produced two satellite peaks around each fundamental reflection. The cross-sections of the respective satellites $\boldsymbol{Q}=(-1,0,2)\pm\boldsymbol{k}$ can be described as follows:[21]

$$I^{\pm}=I_0\{m_{\text{easy}}^2+m_b^2\pm 2m_{\text{easy}}m_b(\boldsymbol{S}_n\cdot\hat{\boldsymbol{q}})\}, \tag{3}$$

where $m_{\text{easy}}=|\boldsymbol{m}_{\text{easy}}|, m_b=|\boldsymbol{m}_b|$, I_0 is a constant, and the caret symbol indicates a unit vector. This cross-section was derived from the approximation that $\boldsymbol{Q}$ was perpendicular to the spiral plane. This approximation had little influence on the quantitative analysis, which is described below since the angles between the normal axis to the spiral plane and the scattering vector $\boldsymbol{Q}=(-1,0,2)\pm\boldsymbol{k}$ was approximately 10° and 16°, respectively. In the case of $\boldsymbol{q}=-\boldsymbol{k}$, the intensities of $(-1,0,2)\pm\boldsymbol{k}$ reflections were calculated by using Eq. (2): $I_p=I_0(m_{\text{easy}}\mp m_b)^2$ and $I_{\text{ap}}=I_0(m_{\text{easy}}\pm m_b)^2$ for $\boldsymbol{S}_n$ parallel and antiparallel to $\boldsymbol{Q}$, respectively. Applying Eq. (1) to each Mn^{2+} zigzag chain, the electric polarization can be calculated as follows:

$$\boldsymbol{P}=+\frac{2A}{V_{\text{cell}}}m_b m_{\text{easy}}e_c\sin\alpha\sin(\pi q_z)\hat{\boldsymbol{b}}. \tag{4}$$

Here, V_{cell} is the volume of the crystallographic unit cell and e_c is the z component of the unit vector connecting Mn_1 to Mn_2. The present neutron study revealed that the left-handed screw $(\boldsymbol{q}=+\boldsymbol{k})$ corresponded to the negatively polarized $(P_b<0)$ domain shown in Fig. 4. The result indicated that the constant A should be negative. Figure 5(a) illustrates the temperature dependence of the integrated polarized-neutron-diffraction intensity of the magnetic satellite at $\boldsymbol{Q}=(-1,0,2)-\boldsymbol{k}$ for the $P_b<0$ state. Equation (3) indicates that $I_p-I_{\text{ap}}\propto m_b m_{\text{easy}}$. The magnetic satellite appeared below T_N but I_p and I_{ap} were almost equivalent because of the sinusoidal collinear spin structure $(m_b=0)$. A difference between them appeared upon the ferroelectric phase transition at T_2 due to the spiral magnetic structure. The difference increased with decreasing temperature and suddenly quenched at T_1 where the spiral structure changed to the commensurate collinear spin structure. In Fig. 5(b), a comparison between the temperature dependence of the observed ferroelectric polarization and the differential intensity of the satellite has been presented. An excellent agreement between them clearly confirmed that the ferroelectric polarization was proportional to $m_{\text{easy}}m_b$ in accordance with the prediction of Eq. (4).

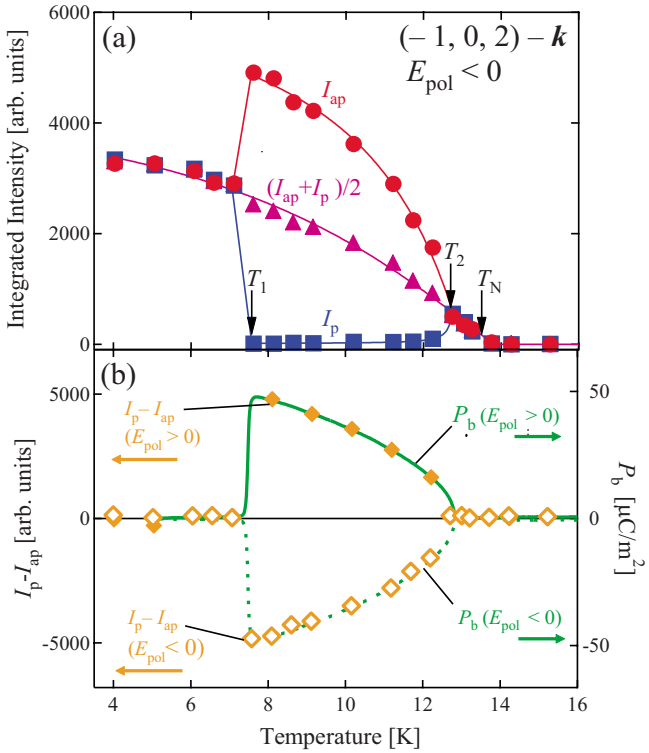

FIG. 5. (Color online) (a) The temperature dependence of the integrated intensities of the magnetic reflection at $(-1,0,2)-k$ in the $E_{\text{pol}}<0$ case. These intensities are corrected by taking into account the imperfect spin polarization of the incident neutron beam. (b) The temperature dependence of the electric polarization and the difference between the integrated intensities I_{ap} and I_p at $Q=(-1,0,2)-k$.

The ellipticity of helix m_b/m_{easy} was also obtained from the intensities I_p and I_{ap}. In fact, the ellipticity at 9 K $(m_b/m_{\text{easy}}=0.9\pm0.1)$ accorded with the result of a previous magnetic structure analysis that revealed that $m_b/m_{\text{easy}}\sim 1$ (Ref. 21). The evolution of m_b/m_{easy} with the temperature in the ferroelectric phase was small in contrast to that in $TbMnO_3$ (Ref. 2). The value of m_b/m_{easy} exceeded 0.7 at 11.8 K. The increase in P mainly originated from the growth of the moment without a significant change in the ellipticity. In $TbMnO_3$, the antiferromagnetic moments along the b axis appeared at 42 K and grew as $T_C(\sim 27$ K) was attained.[2] The c component of the spiral moment and hence the ellipticity, gradually increased below T_C with the evolution of polarization. At 10 K, where P was almost saturated, the spiral was still elliptical with $m_c/m_b\sim 0.7$. The difference between $TbMnO_3$ and $MnWO_4$ can be ascribed to the fact that the

single-ion magnetic anisotropy is considerably larger in $Mn^{3+}(3d^4)$ than in $Mn^{2+}(3d^5)$. The circular shape of the spiral ($m_b/m_{easy} \approx 1$) as well as the absence of $4f$ moments led to a considerably simpler response of $MnWO_4$ to the magnetic fields. In addition, the large magnetic moment enabled the accurate investigation of the static and dynamic magnetic properties of $MnWO_4$, as reported previously.[21,22,26] Recently, the so-called electromagnons, i.e., hybridized magnetic and polar excitations in cycloid multiferroics have attracted a considerable amount of attention (Ref. 27). $MnWO_4$ is possibly one of the best spin systems that can be employed for researches in low-energy physics such as electromagnons in IDM-related multiferroic systems that exhibit a magnetically induced 90° polarization flop.

The present neutron study evidently revealed the strong correlation between spin chirality and electric polarization. The result established the IDM mechanism of ferroelectricity in $MnWO_4$. On the other hand, the spin-orbit coupling did not modulate the ground state of the Mn^{2+} ion with $S=5/2$ and $L=0$ by any means, which was apparently not favorable to the IDM mechanism. The covalency effect that hybridized the $L \neq 0$ component of $Mn^{+}O^{-}$ with the purely ionic $Mn^{2+}O^{2-}$ was probably required to be taken into account. A relatively strong spin-orbit coupling was expected to act as an effective perturbation in both $Mn^{+}(d^6)$ and $O^{-}(p^5)$ states, resulting in the induction of an electric dipole via helical magnetism through a mechanism similar to the IDM interaction.

We thank S. Ohtani and T. Takenobu for their assistance in performing the measurements. This work was partly supported by the Grants-in-Aid for Scientific Research from the Ministry of Education, Culture, Sports, Science, and Technology, Japan.

*Present address: The Department of Earth and Space Science, Graduate School of Science of Osaka University, Osaka 560-0043, Japan.

[1] M. Fiebig, J. Phys. D **38**, R123 (2005).
[2] Y. Yamasaki, H. Sagayama, T. Goto, M. Matsuura, K. Hirota, T. Arima, and Y. Tokura, Phys. Rev. Lett. **98**, 147204 (2007).
[3] T. Kimura, T. Goto, H. Shintani, K. Ishizaka, T. Arima, and Y. Tokura, Nature (London) **426**, 55 (2003).
[4] T. Goto, T. Kimura, G. Lawes, A. P. Ramirez, and Y. Tokura, Phys. Rev. Lett. **92**, 257201 (2004).
[5] T. Kimura, G. Lawes, T. Goto, Y. Tokura, and A. P. Ramirez, Phys. Rev. B **71**, 224425 (2005).
[6] N. Abe, K. Taniguchi, S. Ohtani, T. Takenobu, Y. Iwasa, and T. Arima, Phys. Rev. Lett. **99**, 227206 (2007).
[7] M. Kenzelmann, A. B. Harris, S. Jonas, C. Broholm, J. Schefer, S. B. Kim, C. L. Zhang, S. W. Cheong, O. P. Vajk, and J. W. Lynn, Phys. Rev. Lett. **95**, 087206 (2005).
[8] T. Arima, A. Tokunaga, T. Goto, H. Kimura, Y. Noda, and Y. Tokura, Phys. Rev. Lett. **96**, 097202 (2006).
[9] H. Katsura, N. Nagaosa, and A. V. Balatsky, Phys. Rev. Lett. **95**, 057205 (2005).
[10] I. A. Sergienko and E. Dagotto, Phys. Rev. B **73**, 094434 (2006).
[11] M. Mostovoy, Phys. Rev. Lett. **96**, 067601 (2006).
[12] A. B. Harris, Phys. Rev. B **76**, 054447 (2007).
[13] T. Arima, J. Phys. Soc. Jpn. **76**, 073702 (2007).
[14] G. Lawes, A. B. Harris, T. Kimura, N. Rogado, R. J. Cava, A. Aharony, O. Entin–Wohlman, T. Yildrim, M. Kenzelmann, C. Broholm, and A. P. Ramirez, Phys. Rev. Lett. **95**, 087205 (2005).
[15] T. Kimura, J. C. Lashley, and A. P. Ramirez, Phys. Rev. B **73**, 220401(R) (2006).
[16] Y. Yamasaki, S. Miyasaka, Y. Kaneko, J. P. He, T. Arima, and Y. Tokura, Phys. Rev. Lett. **96**, 207204 (2006).
[17] S. Park, Y. J. Choi, C. L. Zhang, and S. W. Cheong, Phys. Rev. Lett. **98**, 057601 (2007).
[18] Y. Naito, K. Sato, Y. Yasui, Y. Kobayashi, Y. Kobayashi, and M. Sato, J. Phys. Soc. Jpn. **76**, 023708 (2007).
[19] K. Taniguchi, N. Abe, S. Ohtani, H. Umetsu, and Taka-hisa Arima, Appl. Phys. Express **1**, 031301 (2008).
[20] S. Ishiwata, Y. Taguchi, H. Murakawa, Y. Onose, and Y. Tokura, Science **21**, 1643 (2008).
[21] G. Lautenschläger, H. Weitzel, T. Vogt, R. Hock, A. Böhm, M. Bonnet, and H. Fuess, Phys. Rev. B **48**, 6087 (1993).
[22] H. Ehrenberg, H. Weitzel, H. Fuess, and B. Hennion, J. Phys.: Condens. Matter **11**, 2649 (1999).
[23] K. Taniguchi, N. Abe, T. Takenobu, Y. Iwasa, and T. Arima, Phys. Rev. Lett. **97**, 097203 (2006).
[24] A. H. Arkenbout, T. T. M. Palstra, T. Siegrist, and T. Kimura, Phys. Rev. B **74**, 184431 (2006).
[25] M. Blume, Phys. Rev. **130**, 1670 (1963).
[26] H. Ehrenberg, H. Weitzel, H. Fuess, and B. Hennion, J. Phys.: Condens. Matter **11**, 2649 (1999).
[27] See, for example, A. Pimenov, A. A. Mukhin, V. Yu. Ivanov, V. D. Travkin, A. M. Balbashov, and A. Loidol, Nat. Phys. **2**, 97 (2006).